

On the Kohn–Sham density response in a localized basis set

Dietrich Foerster* and Peter Koval†

CPMOH, University of Bordeaux 1

351 Cours de la Liberation, 33405, Talence, France

We construct the Kohn–Sham density response function χ_0 in a previously described basis of the space of orbital products. The calculational complexity of our construction is $O(N^2N_\omega)$ for a molecule of N atoms and in a spectroscopic window of N_ω frequency points. As a first application, we use χ_0 to calculate molecular spectra from the Petersilka–Gossmann–Gross equation. With χ_0 as input, we obtain correct spectra with an extra computational effort that grows also as $O(N^2N_\omega)$ and, therefore, less steeply in N than the $O(N^3)$ complexity of solving Casida’s equations. Our construction should be useful for the study of excitons in molecular physics and in related areas where χ_0 is a crucial ingredient.

PACS numbers: 33.20.-t, 31.15.ee

Keywords: Noninteracting response function, direct solution of Petersilka–Gossmann–Gross equations

I. INTRODUCTION AND MOTIVATION

A basic concept in time-dependent density functional theory [1, 2] is a reference system of noninteracting electrons of the same density $n(\mathbf{r}, t)$ as the interacting electrons under study and moving in an appropriately adjusted potential $V_{\text{KS}}(\mathbf{r}, t)$. Therefore, an important element of this theory is the density response function $\chi_0(\mathbf{r}, \mathbf{r}', t - t')$ that describes the variation in density $\delta n(\mathbf{r}, t)$ of such reference electrons upon a change $\delta V_{\text{KS}}(\mathbf{r}', t')$ of the Kohn–Sham potential

$$\chi_0(\mathbf{r}, \mathbf{r}', t - t') = \frac{\delta n(\mathbf{r}, t)}{\delta V_{\text{KS}}(\mathbf{r}', t')}. \quad (1)$$

The Kohn–Sham density response is needed for implementing Hedin’s GW approximation [4], for electronic excitation spectra [5, 6], for treating excitons in molecular systems [7], and in other contexts, such as the inclusion of the van der Waals interaction in DFT [8]. Various methods have been developed for constructing this response function in solids [9], but for molecules no computationally efficient method has emerged. Therefore, the Kohn–Sham density response

*Electronic address: d.foerster@cpmoh.u-bordeaux1.fr

†Electronic address: koval.peter@gmail.com

remains an important bottleneck in applications of electronic structure methods to molecular physics. In the present paper we describe a solution to this long standing technical problem.

The difficulty of dealing with the noninteracting density response is somewhat surprising, since it can be written down very compactly in terms of molecular orbitals [26]

$$\chi_0(\mathbf{r}, \mathbf{r}', \omega) = \sum_{E, F; EF < 0} \frac{n_F - n_E}{\omega - (E - F) - i\varepsilon(n_E - n_F)} \varphi^E(\mathbf{r}) \varphi^F(\mathbf{r}) \varphi^E(\mathbf{r}') \varphi^F(\mathbf{r}'). \quad (2)$$

Here $\varphi^E(\mathbf{r})$ represents a stationary (real valued) molecular orbital of energy E and n_E is an occupation factor. Although this form of the density response was used very effectively in Casida’s equations for molecular spectra [6], it is less useful, for example, in computing the screening of the Coulomb interaction. In this context, we must integrate over the arguments \mathbf{r}, \mathbf{r}' of $\chi_0(\mathbf{r}, \mathbf{r}', \omega')$ which requires a summation over $O(N^2)$ pairs of points \mathbf{r}, \mathbf{r}' and over $O(N^2)$ energies (E, F) where N is the number of atoms. Therefore, a straightforward application of the conventional expression requires a total of $O(N^4 N_\omega)$ operations. The strong growth of CPU effort with the number of atoms limits the usefulness of expression (2) to molecules or clusters containing very few atoms.

Eq. (2) shows that χ_0 acts in the space of products of molecular orbitals $\varphi^E(\mathbf{r}) \varphi^F(\mathbf{r})$, a space that has no obvious basis. Chemists have long recognized that both the space of products of molecular orbitals and the related space of products of atomic orbitals contain many linearly dependent elements [10]. To eliminate such redundant elements, products of orbitals are usually parametrized in terms of sets of auxiliary functions [6, 11].

In a better controlled and more systematic approach [12] (for a similar method in the context of the GW approach see [13]), one identifies the dominant elements in the space of all products of a given pair of atoms. As a result of this construction, any product of atomic orbitals $f^a(\mathbf{r}), f^b(\mathbf{r})$ can be expanded in a basis of $O(N)$ “dominant functions” $\{F^\mu(\mathbf{r})\}$. In this basis, the density response acts as a frequency dependent matrix $\chi_{\mu\nu}^0(\omega)$

$$\chi_0(\mathbf{r}, \mathbf{r}', \omega) = \sum_{\mu, \nu} F^\mu(\mathbf{r}) \chi_{\mu\nu}^0(\omega) F^\nu(\mathbf{r}'). \quad (3)$$

The present paper describes an efficient construction of this matrix by Green’s function type methods that require $O(N^2 N_\omega)$ operations for a molecule of N atoms and in a spectroscopic window of N_ω frequency points.

To test this construction, we apply it to electronic excitation spectra of molecules, where many results are known. We consider two approaches for excitation spectra: the Petersilka–Gossmann–Gross equations [5] and Casida’s equations [6]. The test of χ_0 on molecular spectra turns out to be successful as our spectra agree indeed with those found from Casida’s equation.

Our paper is organized as follows: in section II we derive a spectral representation of χ_0 and discuss its locality properties. In section III, we formulate and test an algorithm that exploits the spectral representation of χ_0 . In section IV, we further test χ_0 by applying it to the computation of electronic excitation spectra. To accelerate the computation, we develop an iterative Lanczos-like procedure. Section V gives our conclusions.

II. A SPECTRAL REPRESENTATION FOR THE KOHN–SHAM DENSITY RESPONSE

Extended versus local fermions

Our approach is based on Green's functions and their spectral functions. So let us recall some of their basic definitions [3] and establish our notation [27]. In the framework of second quantization, the electronic propagator reads

$$iG(\mathbf{r}, \mathbf{r}', t - t') = \langle 0 | T \{ \psi(\mathbf{r}, t) \psi^\dagger(\mathbf{r}', t') \} | 0 \rangle = \theta(t - t') \langle 0 | \psi(\mathbf{r}, t) \psi^\dagger(\mathbf{r}', t') | 0 \rangle - \theta(t' - t) \langle 0 | \psi^\dagger(\mathbf{r}', t') \psi(\mathbf{r}, t) | 0 \rangle, \quad (4)$$

where ψ and ψ^\dagger are annihilation and creation operators of electrons, respectively. The symbol T represents time ordering of operators and $\theta(t)$ is the unit step function.

According to general principles [3], the density response function (1) coincides with the density–density correlator of the unperturbed system

$$i\chi_0(\mathbf{r}, \mathbf{r}', t - t') = \langle 0 | T \{ n(\mathbf{r}, t) n(\mathbf{r}', t') \} | 0 \rangle, \quad (5)$$

where $n = \psi^\dagger \psi$ is the electronic density operator. For simplicity, we mostly use the time ordered form of correlators, the Fourier transform of which coincides with that of the causal one at positive frequencies. For noninteracting electrons, the density response can be expressed in terms of electron propagators $G(\mathbf{r}, \mathbf{r}', t - t')$. Applying Wick's theorem [3] on eq. (5), we find

$$i\chi_0(\mathbf{r}, \mathbf{r}', t - t') = G(\mathbf{r}', \mathbf{r}, t - t') G(\mathbf{r}', \mathbf{r}, t' - t), \quad (6)$$

where we ignore the time-independent (disconnected) part of the correlator that contributes to the response only at zero frequency.

To confirm the conventional expression for χ_0 in terms of molecular orbitals (2), we expand the operators $\psi(\mathbf{r}, t)$ in terms of Kohn–Sham orbitals $\varphi_E(\mathbf{r})$ and their associated fermion operators $c_E(t)$

$$\psi(\mathbf{r}, t) = \sum_E \varphi_E(\mathbf{r}) c_E(t). \quad (7)$$

We use the last expression to rewrite the Green’s function (4) in terms of molecular orbitals

$$G(\mathbf{r}, \mathbf{r}', t - t') = -i\theta(t - t') \sum_{E>0} \varphi_E(\mathbf{r}) \varphi_E(\mathbf{r}') e^{-iE(t-t')} + i\theta(t' - t) \sum_{E<0} \varphi_E(\mathbf{r}) \varphi_E(\mathbf{r}') e^{-iE(t-t')}, \quad (8)$$

where we took into account the anticommutator $[c_E(t), c_{E'}^\dagger(t)]_+ = \delta_{E,E'}$, the time evolution $c_E(t) = e^{-iEt} c_E(0)$ and the nature of the ground state. Regularizing the above expression with a damping factor $e^{-\varepsilon(t-t')/2}$, using (8) in eq. (6) and doing a Fourier transform on the result, we easily confirm the textbook expression eq. (2) for χ_0 .

Our approach emphasizes locality and it is better to use a localized basis of atomic orbitals $f^a(\mathbf{r})$. Therefore, we write the molecular orbitals as linear combinations of atomic orbitals (LCAO)

$$\varphi_E(\mathbf{r}) = \sum_a X_a^E f^a(\mathbf{r}). \quad (9)$$

Here X_a^E are (generalized) eigenvectors of the Kohn-Sham Hamiltonian labelled by their eigenvalues E . Inserting the latter expression in equation (8), we obtain the propagator in the localized basis. For later convenience, we write this result in terms of spectral functions of particles and holes

$$G_{ab}(t) = -i\theta(t) \int_0^\infty ds \rho_{ab}^+(s) e^{-ist} + i\theta(-t) \int_{-\infty}^0 ds \rho_{ab}^-(s) e^{-ist}. \quad (10)$$

Here, we introduced the spectral densities of particles and holes

$$\rho_{ab}^+(s) = \sum_{E>0} X_a^E X_b^E \delta(s - E) \quad \text{and} \quad \rho_{ab}^-(s) = \sum_{E<0} X_a^E X_b^E \delta(s - E). \quad (11)$$

Definition of a frequency dependent response matrix

Let us also write the operators $\psi(\mathbf{r}, t)$ in terms of localized atomic orbitals with localized fermion operators $c_a(t)$ as coefficients [14]. We have

$$\psi(\mathbf{r}, t) = \sum_a f^a(\mathbf{r}) c_a(t) \quad (12)$$

with $c_a(t) = \sum_E X_a^E c_E(t)$. Because we use local orbital fermions (12), the electron density $n(\mathbf{r}, t)$ is given by a sum over products of orbitals multiplied by bilinears of fermion operators

$$n(\mathbf{r}, t) = \psi^\dagger(\mathbf{r}, t) \psi(\mathbf{r}, t) = \sum_{a,b} f^a(\mathbf{r}) f^b(\mathbf{r}) c_a^\dagger(t) c_b(t). \quad (13)$$

It is well known that the set of products of orbitals contains collinear or nearly collinear elements, a fact nicely illustrated by taking products of the eigenfunctions (Hermite functions) of the harmonic oscillator [10]. Traditionally, this difficulty is treated by expanding products of orbitals in auxiliary functions.

In a recent and more systematic approach [12], one identifies a set of “dominant products” $\{F^\lambda(\mathbf{r})\}$ as special linear combinations in the space of products of orbitals. A similar method was previously developed in the context of the GW method [13]. The main collinearity of the set of orbital products occurs at the level of a fixed pair of atoms. Therefore all the products $f^a(\mathbf{r}) \cdot f^b(\mathbf{r})$ belonging to such a fixed pair were formed. A matrix of overlaps between these products was computed and the dominant products were found among the linear combinations of the original products that diagonalize this matrix. As a result, all nonzero orbital products can be expressed in terms of a much smaller set of dominant products

$$f^a(\mathbf{r})f^b(\mathbf{r}) = \sum_{\lambda} V_{\lambda}^{ab} F^{\lambda}(\mathbf{r}). \quad (14)$$

This is done without any extra fitting functions and with an accuracy that appears to increase exponentially with the number of basis functions. The notation $F^\lambda(\mathbf{r})$ alludes to the eigenvalue λ that is related to the norm of these functions. Combining eqs. (13, 14), we may express the density operator as

$$n(\mathbf{r}, t) = \psi^+(\mathbf{r}, t)\psi(\mathbf{r}, t) = \sum_{a,b,\mu} F^{\mu}(\mathbf{r})c_a^{\dagger}(t)V_{\mu}^{ab}c_b(t). \quad (15)$$

Inserting this representation of the density into eq. (5), we find a representation of the density correlator as a sum of products of dominant functions

$$i\chi_0(\mathbf{r}, \mathbf{r}', t - t') = \sum_{\mu,\nu} F^{\mu}(\mathbf{r}) \chi_{\mu\nu}^0(t - t') F^{\nu}(\mathbf{r}'). \quad (16)$$

The entries of the matrix $\chi_{\mu\nu}^0$ are correlators of bilinears of local fermions

$$\begin{aligned} i\chi_{\mu\nu}^0(t - t') &= \sum_{iklm} \langle 0|T\{c_i^{\dagger}(t)V_{\mu}^{ik}c_k(t) \cdot c_l^{\dagger}(t)V_{\nu}^{lm}c_m(t')\}|0\rangle \\ &= \text{Tr}(V_{\mu}G(t - t')V_{\nu}G(t' - t)). \end{aligned} \quad (17)$$

In this equation, the explicit expression in terms of Green’s functions was found again with the help of Wick’s theorem. Equation (17) describes the creation, propagation and subsequent annihilation of a particle hole pair, see figure 1. The figure shows why the construction of $\chi_{\mu\nu}^0$ requires $O(N^2N_{\omega})$ operations. There are $O(N)$ dominant products for the entire molecule, and there are a total of $O(N^2)$ pairs of such products. Due to the locality of the

vertex V_{μ}^{ab} , there are, for each pair, of order $O(N^0)$ electron propagators to be summed over. Finally, the calculation must be done for N_{ω} frequencies.

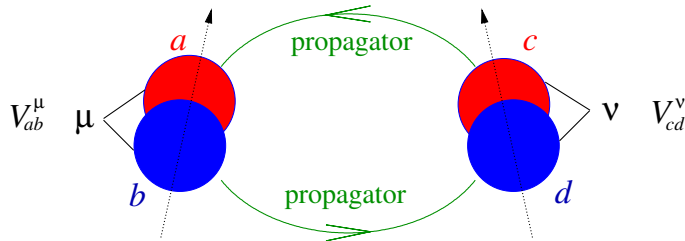


FIG. 1: Particle hole graph for χ_0 in a basis of dominant products. The vertex V_{ab}^{μ} connects pairs of orbitals a, b to a dominant product μ . The propagators connect the orbitals within the orbital quadruplet. For a given pair of dominant products (μ, ν) , there are $O(N^0)$ orbitals to be summed over. Therefore, the total computational effort scales as $O(N^2 N_{\omega})$.

Finding the spectral function of $\chi_{\mu\nu}^0(\omega)$

It would be a mistake to determine χ_0 directly, on the basis of eq. (17), by brute force computation. At equal times, the electron propagator has a discontinuity which hampers such an approach. Instead, it is better to relate the density response χ_0 and the electron propagators G indirectly via their spectral functions and to construct $\chi_{\mu\nu}^0$ from its spectral density at the end.

The Fourier transform of the causal (rather than the time ordered) form of $\chi_{\mu\nu}^0$ is analytic in the cut complex plane. Therefore, it should have the following Cauchy type spectral representation

$$\chi_{\mu\nu}^0(\omega + i\varepsilon) = \frac{1}{\pi} \int_{-\infty}^{\infty} \frac{\text{Im}\chi_{\mu\nu}^0(s) ds}{\omega + i\varepsilon - s}. \quad (18)$$

Once we know that such a representation should exist, it is easy to identify the spectral density by combining eqs. (10,11,17). After a brief calculation, we obtain the following result

$$i\chi_{\mu\nu}^0(\omega) = \int_0^{\infty} d(\lambda^2) \frac{a_{\mu\nu}(\lambda)}{(\omega + i\varepsilon)^2 - \lambda^2}; \quad (19)$$

$$a_{\mu\nu}(\lambda) = \int \int_0^{\infty} d\sigma d\tau \text{Tr} [V_{\mu}\rho^+(\sigma)V_{\nu}\rho^-(-\tau)] \delta(\sigma + \tau - \lambda) \text{ for } \lambda > 0. \quad (20)$$

The first line shows that the response matrix $\chi_{\mu\nu}^0(\omega)$ can be computed from the spectral function $a_{\mu\nu}(\lambda)$. The second line shows that this spectral function is a weighted convolution of particle like (+) and hole like (-) spectral densities (11). Eqs. (19, 20) are the basis of our algorithm for evaluating the response matrix $\chi_{\mu\nu}^0(\omega)$ in the next section.

III. COMPUTATION OF χ_0 FROM ELECTRONIC SPECTRAL DENSITIES

To compute the convolutions in eq. (20) efficiently, we make extensive use of the fast Fourier transform that does such convolutions in $O(N_\omega \log N_\omega)$ operations for N_ω frequency points [15]. In this section, we will explain (i) how to discretise the electronic spectral density on a frequency lattice and (ii) how to evaluate the spectral integral over the infinite frequency interval in eq. (19).

Discretizing the spectral density

We will discretize the electronic spectral densities in eq. (11) in a window $(-\omega_{\max}, \omega_{\max})$ and on a grid with spacing $\Delta\omega = \frac{\omega_{\max}}{N_\omega}$. To hide the effect this might have on $\chi_{\mu\nu}^0(\omega)$ we will later broaden the spectral resolution by adding a small imaginary part $i\varepsilon$ to the frequency. Let the grid points be defined as follows

$$\omega_n = \frac{n}{N_\omega}\omega_{\max}, \Delta\omega = \frac{\omega_{\max}}{N_\omega}, n = 1 - N_\omega \dots N_\omega - 1. \quad (21)$$

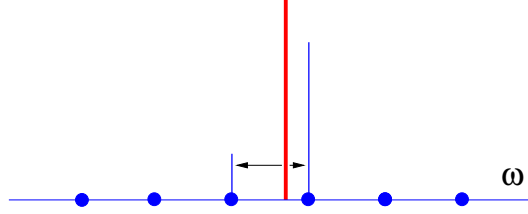


FIG. 2: Redistribution of spectral weight on the frequency mesh.

Consider an eigenenergy E that belongs to the frequency window $-\omega_{\max} < E < \omega_{\max}$ [28] and which is located between two successive mesh points (ω_n, ω_{n+1}) . We distribute the spectral weight $X_a^E X_b^E$ to the neighboring frequencies ω_n, ω_{n+1} in a way that conserves (i) the total spectral weight and (ii) it's center of mass by using the following weight factors p_n, p_{n+1}

$$p_n = \frac{\omega_{n+1} - E}{\Delta\omega}, \quad p_{n+1} = 1 - p_n. \quad (22)$$

Alternatively, one may also minimize the norm of the difference Δ between the pole at $\omega = E$ and its representation by poles at the two neighboring frequencies on the lattice

$$\Delta(\omega) = \frac{p_n}{\omega - (\omega_n + i\varepsilon)} + \frac{p_{n+1}}{\omega - (\omega_{n+1} + i\varepsilon)} - \frac{1}{\omega - (E + i\varepsilon)} \equiv \sum_{i=n, n+1, 0} \frac{p_i}{\omega - \omega_i + i\varepsilon}, \quad (23)$$

$$p_0 = -1, \quad p_{n+1} = 1 - p_n, \quad \omega_0 = E.$$

There is a simple expression for the norm of this error that can be obtained by contour integration

$$\|\Delta\|^2 = \frac{1}{2\pi} \int_{-\infty}^{\infty} |\Delta(\omega)|^2 d\omega = 2\varepsilon \sum_{i,k=n,n+1,0} \frac{p_i p_k}{(\omega_i - \omega_k)^2 + 4\varepsilon^2}. \quad (24)$$

With $\varepsilon \gtrsim \Delta\omega$, the coefficient p_n , that minimizes the error norm, varies almost linearly between 0 and 1 as a function of $\frac{E}{\Delta\omega}$ and differs little from eq. (22). As the errors are of the same order in both cases, we use the first and simpler method according to eq. (22). This part of the calculation actually requires $O(N^3)$ operations, but the prefactor is very small – the discretization of the spectral data of benzene takes about a second on a current PC.

To judge the quality of this discretisation, we compute the density of states $-\frac{1}{\pi}\text{Tr}(S \text{Im} G(\omega + i\varepsilon))$ in the case of benzene, within a window of frequencies (i) by direct calculation from the exact Green's function and (ii) after redistributing the spectral weights. Figure 3 shows that the two densities of states differ very little. The good agreement between the two densities vindicates our discretization procedure.

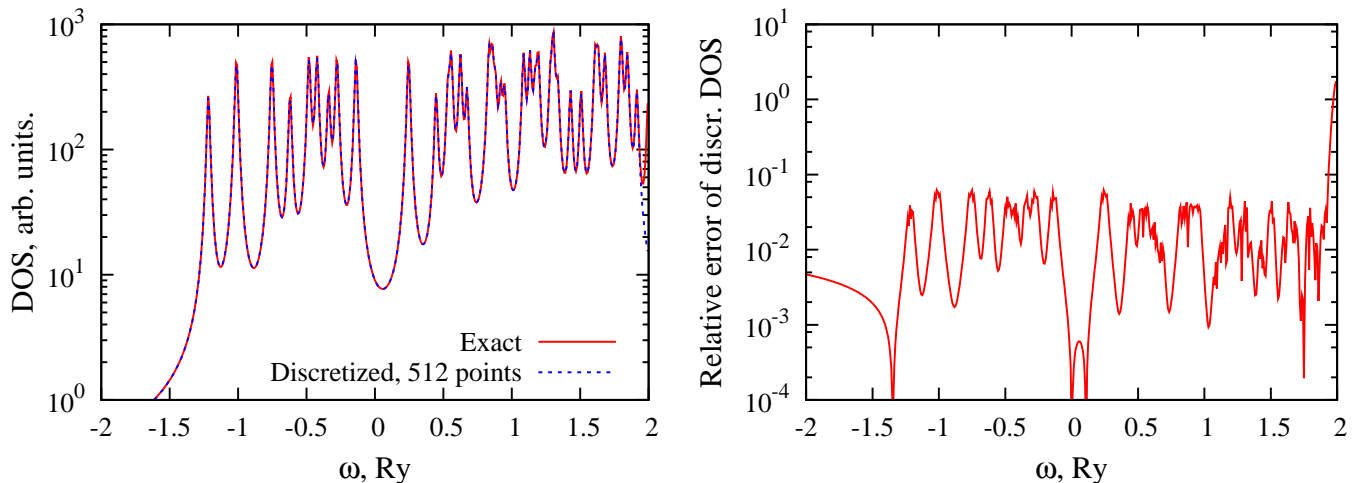


FIG. 3: The (noninteracting) density of states (DOS) of benzene. The exact DOS $\sum_E(\omega - E + i\varepsilon)^{-1}$ is computed with eigenvalues E obtained using the Siesta package [16]. Default settings were used in the Siesta run. The discretized DOS is computed in the frequency window $-\omega_{\max} < \omega < \omega_{\max}$, $\omega_{\max} = 2$ Rydberg with $N_\omega = 512$ data points. ε is chosen to be $1.5\Delta\omega$, where the discretisation spacing is $\Delta\omega = 2\omega_{\max}/N_\omega$.

The need for a second spectral window

According to eq. (19) we must find an integral over the full spectral range $(0, \Omega_{\max})$ even if we want spectroscopic results only for low frequencies $\omega \leq \omega_{\max}$. We resolve this difficulty by decomposing the integral in eq. (19) as follows

$$\begin{aligned} \chi_{\mu\nu}^0(\omega) &= \left(\int_0^{\omega_{\max}} + \int_{\omega_{\max}}^{\Omega_{\max}} \right) a_{\mu\nu}(\lambda) \left(\frac{1}{\omega + i\varepsilon - \lambda} - \frac{1}{\omega + i\varepsilon + \lambda} \right) d\lambda \\ &\equiv \chi_{\mu\nu}^{0, \text{resonant}}(\omega) + \chi_{\mu\nu}^{0, \text{nonresonant}}(\omega). \end{aligned} \quad (25)$$

The first term $\chi_{\mu\nu}^{0, \text{resonant}}$ in this decomposition has resonant structure because ω and λ may coincide in the denominator of its integrand. By contrast, the integrand in the expression for $\chi_{\mu\nu}^{0, \text{nonresonant}}$ is regular and therefore this function has much less structure. For the resonant part, we must allow for sufficiently many grid points to capture the features of the spectral density. For the nonresonant part, we determine the spectral density for the full range of Kohn–Sham eigenvalues, and for simplicity, we use the same number of gridpoints N_ω . However, we need the resulting response function $\chi_{\mu\nu}^{0, \text{nonresonant}}(\omega)$ only in the frequency interval $(0, \omega_{\max})$ where we find its values on the corresponding grid points (21) by interpolation.

To judge the quality of $\chi_{\mu\nu}^0(\omega)$ constructed in this way, we make use of the exact expression (2) for the response function. The corresponding response matrix $\chi_{\mu\nu}^{0, \text{exact}}(\omega)$ can be obtained by expressing $\varphi_E(\mathbf{r})\varphi_F(\mathbf{r})$ in eq. (2) in terms of dominant functions. Using eqs. (2,9,14) we obtain

$$\chi_{\mu\nu}^{0, \text{exact}}(\omega) = \sum_{EF < 0; a, b, c, d} \frac{n_F - n_E}{\omega - (E - F) - i\varepsilon(n_E - n_F)} (X_a^E V_\mu^{ab} X_b^E) (X_c^F V_\nu^{cd} X_d^F). \quad (26)$$

Actually, the exact response matrix $\chi_{\mu\nu}^{0, \text{exact}}(\omega)$ requires $O(N^4 N_\omega)$ and it takes too long to compute for other than very small molecules. Nonetheless, the exact expression (26) is well suited as a test provided we use it only for fixed entries μ, ν . Figure 4 indicates that the error is well controlled and vindicates our “two windows technique” for constructing $\chi_{\mu\nu}^0(\omega)$.

We argued before that the total computational cost of our method scales as $O(N^2 N_\omega)$ and we believe that this scaling is the best that can be achieved for the noninteracting response function χ_0 . In order to confirm this scaling, we computed the noninteracting response χ_0 for a number of carbon chains, measured the wall clock time and represented it in figure 5. The scaling law is slightly disturbed, probably due to the high memory requirement of our algorithm in the case of the C_{18} chain.

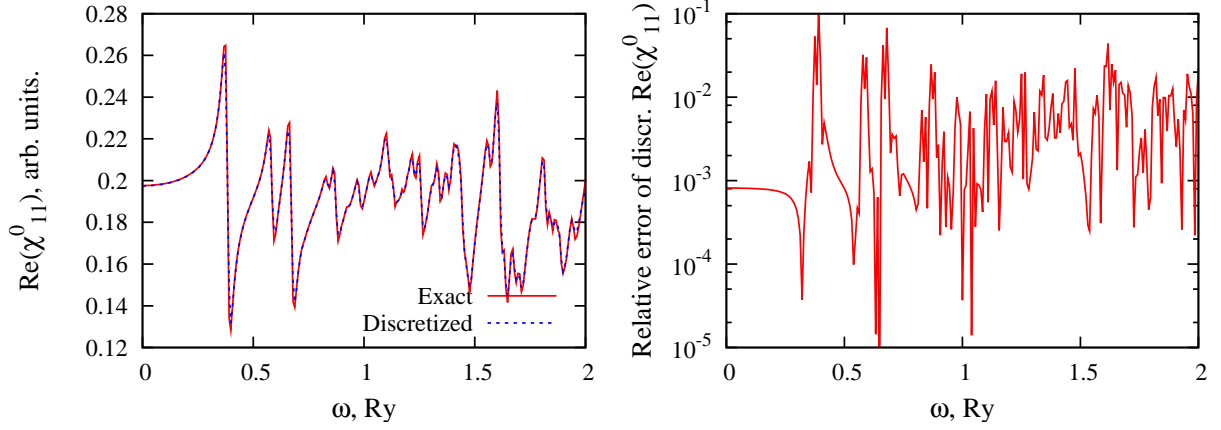


FIG. 4: An element of the response function $\chi_{\mu\nu}^0$ of benzene. The exact response is computed according to eq. (26). The Kohn–Sham eigenstates were generated using the Siesta package [16] with default settings. The discretized response function is computed in the frequency window $\omega < \omega_{\max}$, $\omega_{\max} = 2$ Rydberg with $N_\omega = 512$ data points. ε is chosen to be $1.5\Delta\omega$, where the discretisation spacing is $\Delta\omega = 2\omega_{\max}/N_\omega$.

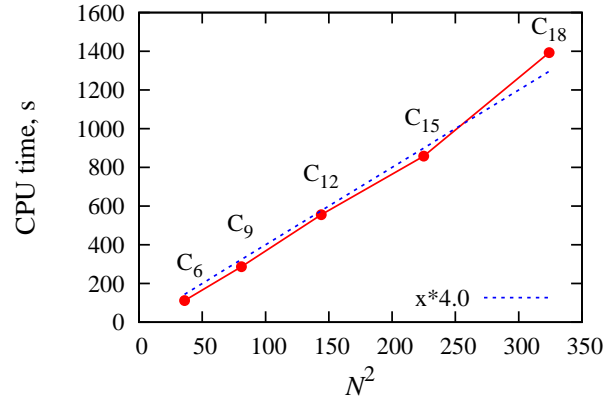


FIG. 5: CPU time for computing χ_0 as a function of the number of atoms N in the case of carbon chains.

IV. TESTING χ_0 IN THE CALCULATION OF MOLECULAR SPECTRA

The Petersilka–Gossmann–Gross equation

In the previous section, we gave a first test of our construction of $\chi_{\mu\nu}^0$ by comparing with an exact result. Here we will further test $\chi_{\mu\nu}^0$ by using it to compute molecular spectra from the Petersilka–Gossmann–Gross equations of

TDDFT linear response [5]

$$\chi^{-1}(\mathbf{r}, \mathbf{r}', \omega) = \chi_0^{-1}(\mathbf{r}, \mathbf{r}', \omega) - f_{\text{H}}(\mathbf{r}, \mathbf{r}') - f_{\text{xc}}(\mathbf{r}, \mathbf{r}'); \quad (27)$$

$$P_{ik}(\omega) = \int d\mathbf{r} d\mathbf{r}' r_i \chi(\mathbf{r}, \mathbf{r}', \omega) r'_k. \quad (28)$$

The results will be compared with spectra obtained using Casida’s equations [6]. The Petersilka–Gossmann–Gross equations are a consequence of a generalisation of the Kohn–Sham equations of the electron gas [17] to time dependent electron densities

$$V_{\text{KS}}(\mathbf{r}, t) = V_{\text{ext}}(\mathbf{r}, t) + V_{\text{H}}(\mathbf{r}, t) + V_{\text{xc}}(\mathbf{r}, t). \quad (29)$$

Here $V_{\text{KS}}(\mathbf{r}, t)$ is the potential that assures a prescribed density $n(\mathbf{r}, t)$ of the noninteracting Kohn–Sham reference electrons, $V_{\text{H}}(\mathbf{r}, t) = 2 \int \frac{n(\mathbf{r}', t)}{|\mathbf{r} - \mathbf{r}'|} d\mathbf{r}'$ (the factor 2 is from spin) and $V_{\text{xc}}(\mathbf{r}, t)$ is the exchange correlation potential. All quantities in this equation depend on the electronic density $n(\mathbf{r}, t)$. We differentiate both sides with respect to this density and upon using $\chi_0 = \frac{\delta n}{\delta V_{\text{KS}}}$, $\chi = \frac{\delta n}{\delta V_{\text{ext}}}$ we obtain equation (27) with the following kernels

$$f_{\text{H}} = 2 \frac{\delta(t - t')}{|\mathbf{r} - \mathbf{r}'|} \quad \text{and} \quad f_{\text{xc}} = \frac{\delta V_{\text{xc}}(\mathbf{r}, t)}{\delta n(\mathbf{r}', t')}. \quad (30)$$

We make the conventional “adiabatic” assumption that f_{xc} has no memory and that it depends only on the instantaneous electron density. Therefore, both f_{H} and f_{xc} are local in time and their Fourier transforms are frequency independent.

In the last section, we computed $\chi_0 = \frac{\delta n}{\delta V_{\text{KS}}}$. In the next subsections we will compute the kernels f_{H} , f_{xc} and the polarizability $P_{ik}(\omega)$.

Computing the kernels f_{H} and f_{xc} in a basis of dominant products

In the basis of dominant products, the Hartree part of the kernel reads

$$f_{\text{H}}^{\mu\nu} = \int d\mathbf{r} d\mathbf{r}' F^{\mu}(\mathbf{r}) \frac{1}{|\mathbf{r} - \mathbf{r}'|} F^{\nu}(\mathbf{r}'). \quad (31)$$

For the present discussion to be reasonably self contained, we must give more details on the structure of the dominant products [12]. As seen previously in section II, the dominant products were constructed in the context of the LCAO method where molecular orbitals are expanded as linear combinations of atomic orbitals (9). Therefore, orbital products and the dominant products constructed from them have either spherical or only axial symmetry depending on whether the two atoms that give rise to them coincide or not. Technically, the products are represented as

expansions in spherical harmonics (in appropriate local coordinates, if necessary) about a midpoint between the two atoms that form the pair.

The Hartree kernel $f_{\text{H}}^{\mu\nu}$ involves two products $F^\mu(\mathbf{r})$, $F^\nu(\mathbf{r})$ that belong, generally, to two distinct pairs of atoms with their own axial or spherical symmetry and local coordinates. With the help of Wigner’s rotation matrices $d_{mm'}^j$ [18] the two distinct products can be referred to a single reference frame. In the end, the Hartree kernel is reduced to a sum of conventional two center integrals

$$\int d\mathbf{r}_1 d\mathbf{r}_2 g_{j_1 m_1}(\mathbf{r}_1 - \mathbf{c}_1) \frac{1}{|\mathbf{r}_1 - \mathbf{r}_2|} g_{j_2 m_2}(\mathbf{r}_2 - \mathbf{c}_2), \quad (32)$$

where the elementary functions $g_{jm}(\mathbf{r}) = g_j(r)S_{jm}(\mathbf{r})$ are explicitly of spherical symmetry [29].

The calculation of such conventional two center integrals is conveniently done in momentum space and using Talman’s fast Bessel transform [19] to relate real space orbitals to their Fourier images.

Due to the finite support of the dominant products, the Hartree kernel must be integrated explicitly only for a subset of $O(N)$ pairs of mutually overlapping dominant products. The Coulomb interaction of the remaining nonoverlapping pairs of products can be calculated exactly and cheaply as an interaction between their multipoles.

By contrast, the remaining kernel f_{xc} is a 3-dimensional integral in the local density approximation

$$f_{\text{xc}}^{\mu\nu} = \int d\mathbf{r} F^\mu(\mathbf{r}) \frac{dV_{\text{xc}}}{dn} F^\nu(\mathbf{r}). \quad (33)$$

There are only $O(N)$ such matrix elements to calculate because the basis functions $F^\mu(\mathbf{r})$ have finite support. In the general case, the integration domain is an overlap of two distinct lenses because the support of each dominant product is an overlap of two spheres. In spite of this, we used a simple numerical integration in spherical coordinates as an easy alternative to more elaborate integration techniques, with the center of spherical coordinates on the midpoint between the two centers, each associated with a dominant product. The integration over solid angle is done via Lebedev’s method [20]. and integration over the radial coordinates is done by the Gauss–Legendre method. By default, we use 86 grid points in Lebedev integration and 24 grid points in Gauss–Legendre integration.

Finding the molecular polarizability

Solving eq. (27) in the basis of dominant products, we find the interacting polarizability $P_{ik}(\omega)$

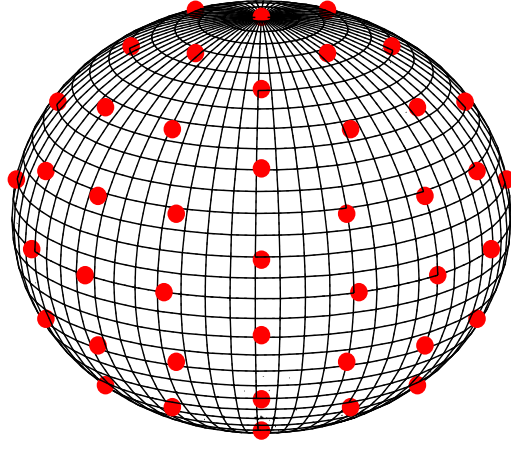


FIG. 6: The nodes of a Lebedev grid with 86 points. With this grid we can exactly integrate any linear combination of spherical harmonics up to angular momentum $j = 15$.

$$P_{ik}(\omega) = \mathbf{d}_i \chi \mathbf{d}_k = \mathbf{d}_i \frac{1}{1 - \chi_0(\omega)f} \chi_0(\omega) \mathbf{d}_k, \quad (34)$$

$$\mathbf{d}_i^\mu = \int d\mathbf{r} \, r_i F^\mu(\mathbf{r}).$$

Here \mathbf{d}^μ is a vector of dipole moments that is associated with the dominant products $F^\mu(\mathbf{r})$. One way compute the polarizability (34) by matrix inversion or, alternatively, by solving N linear equations in N variables to find $\chi \mathbf{d}_k$. Either method requires $O(N^3 N_\omega)$ operations which is worse than the $O(N^2 N_\omega)$ scaling in the computation of χ_0 . On the other hand, equation (34) shows that the polarizability does not see the full matrix χ but only its (low rank) projection onto the dipole moments \mathbf{d} . Fortunately, iterative Lanczos–Krylov methods [21] are capable of finding such projections of the inverse of a matrix in $O(N^2)$ operations.

To find the inverse of a matrix $A = 1 - \chi_0(\omega)f$ contracted with two vectors $\langle L| = \mathbf{d}_i$ and $|R\rangle = \chi_0(\omega)\mathbf{d}_i$, we use a biorthogonal Lanczos construction based on the two sets of Krylov spaces $\{A^n|R\rangle\}$, $\{\langle L|A^n\}$. This construction provides us with (i) a set of orthonormal states $\langle n|m\rangle = \delta_{mn}$, with (ii) a tridiagonal representation of A and (iii) with an easily calculable inverse of A within the Krylov spaces $\{A^n|R\rangle\}$, $\{\langle L|A^n\}$

$$A \sim \sum_{m,n} |m\rangle t_{mn} \langle n| \text{ and } A^{-1} \sim \sum_{m,n} |m\rangle t_{mn}^{-1} \langle n| \quad (35)$$

(we wrote “ \sim ” because the construction is at most asymptotic). We find the following representation of the trace of

the polarizability (relevant when averaging over directions)

$$\begin{aligned} \frac{1}{1 - \chi_0(\omega)f} &= \sum |m\rangle t_{mn}^{-1} \langle n|, \\ P_{ii}(\omega) &= \langle L|1\rangle t_{11}^{-1} \langle 1|R\rangle = t_{11}^{-1} P_{ii}^0(\omega). \end{aligned} \quad (36)$$

The relation $\langle L|1\rangle \langle 1|R\rangle = \langle L|R\rangle = P_{ii}^0(\omega)$ is a simple normalization condition that follows also from the biorthogonality of the Lanczos vectors. Equation (36) shows that the interaction causes the Kohn–Sham polarizability to be multiplied by a factor that is the (1,1) component of the inverse of the matrix t^{-1} . With a small Krylov dimension of $O(N^0)$, the calculational effort scales as $O(N^2)$ [30].

If the full polarization tensor P_{ik} is wanted, then it is better to use a block Lanczos procedure [21]. We then consider the following Krylov spaces and biorthogonalize them

$$\langle L, i |_{i=1..3} A^n \quad \text{and} \quad A^n |R, i\rangle_{i=1..3} \quad (37)$$

where $|R, i\rangle$ and $\langle L, i|$ represent, respectively, $\chi_{\mu\nu}^0(\omega) d_i^\nu$ and d_i^μ . The scalar representation (36) is now replaced by the following block representations of $(1 - \chi_0(\omega)f)^{-1}$

$$\frac{1}{1 - \chi_0 f} \sim \sum |m, i\rangle t_{mi,nk}^{-1} \langle n, k|. \quad (38)$$

Applying this to $P_{ik}(\omega)$ we found

$$P_{ik}(\omega) \sim \sum_{ab} \langle L, i | 1, a\rangle (t^{-1})_{1a,1b} \langle 1, b | R, k\rangle. \quad (39)$$

We chose to keep the left vectors at the lowest Krylov level unchanged and obtain $\langle 1, a | 1, b\rangle = \delta_{ab}$ as a normalization condition. We therefore find the following simple matrix relation between $P(\omega)$ and $P_0(\omega)$

$$P(\omega) = (t^{-1})_{11} P_0(\omega).$$

The details of the block Lanczos algorithm [21] are not given here. They are standard and may be obtained from the authors upon request.

Electronic excitation spectra of molecules

In the previous section, we described a numerical procedure for calculating the dynamical polarizability $P_{ik}(\omega)$ in $O(N^2 N_\omega)$ operations. Our implementation of this algorithm contains a number of computational parameters that

have to be adjusted properly. For instance, the precision of our Lanczos method depends on the dimension of its Krylov space. In the examples below, a very small Krylov dimension $\lesssim 10$ gave a polarization $P(\omega)$ with a relative error of $\lesssim 10^{-2}$. Other computational parameters were carefully cross checked and the results of some of these calculations are given in the figures 3 and 4.

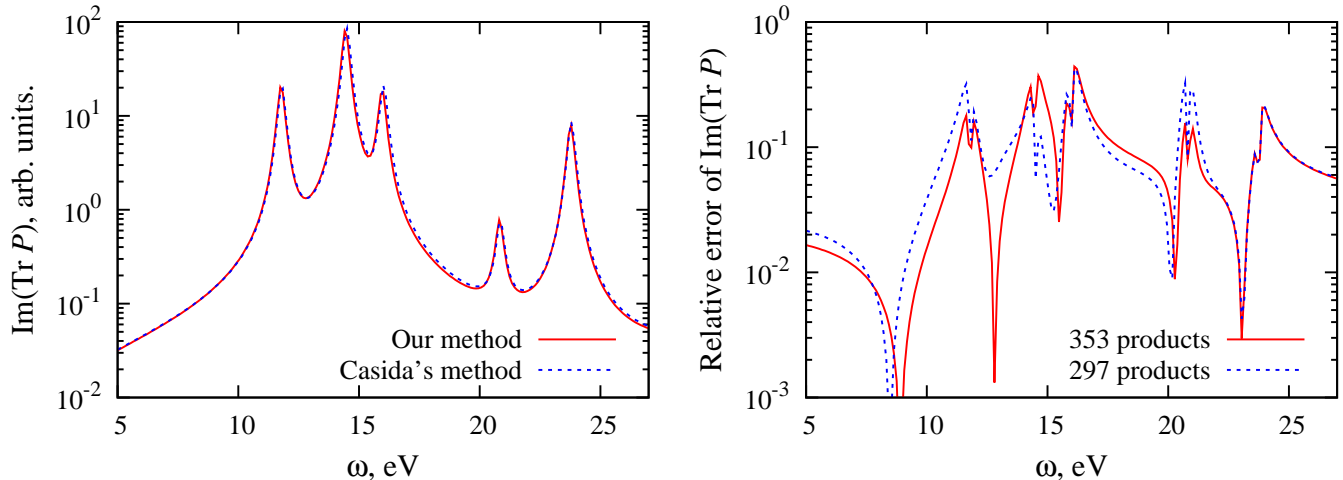


FIG. 7: Polarizability calculated by our method and compared with that of Casida. The methane molecule is computed with deMon2k’s default basis set (DZVP); the Perdew–Zunger exchange–correlation potential has been used.

In order to test the method as a whole, we compared our polarizabilities with those computed from Casida’s equations [6] with the help of the deMon2k package [22]. Casida’s equations allow the determination of excitation energies ω_I and corresponding oscillator strengths f_I and provide a dynamical polarizability that is parametrized as

$$\frac{1}{3}\text{Tr}P(\omega) = \frac{1}{3} \sum_I \frac{f_I}{(\omega + i\varepsilon)^2 + \omega_I^2}.$$

We successfully compared results for several small molecules: hydrogen, methane, methane dimer, benzene and diborane. The results of the two methods for methane are presented in figure 7 where we see a reasonable agreement. To achieve this agreement we had to discretize the basis orbitals (contracted Gaussians in deMon2k) on our numerical grid and import them into our code. In all the cases, our results converged to those of Casida when we enlarge our basis of dominant products. However, a large number of dominant products is needed in order to achieve convergence. For instance, we had to take about 360 dominant products in case of methane and more than 1800 in case of benzene. This is due to the comparatively large support of the Gaussian basis in deMon2k. Therefore, in the next example, we used a basis of numerical atomic orbitals which is far more natural for our method.

Numerical orbitals of compact support were taken from the Siesta package [16]. Their support is 4...6 bohr which is about two to three times smaller than the effective limit chosen for the support of deMon2k’s orbitals. This allows to

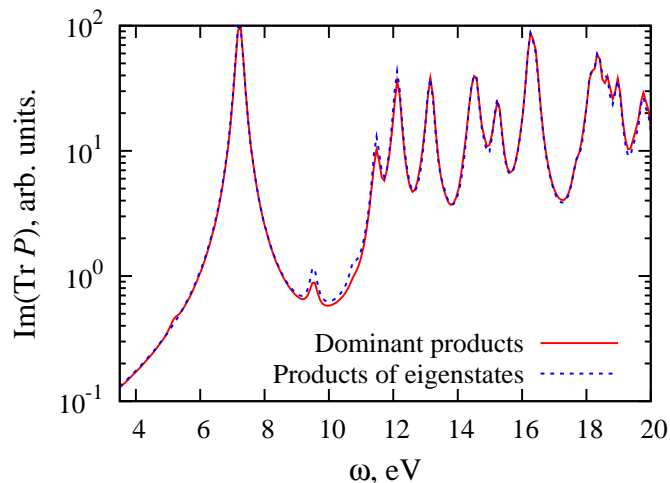


FIG. 8: Spectra of benzene computed in basis of dominant products and in basis of products of eigenstates. Kohn–Sham eigenstates have been imported from the Siesta package [16]. Default settings were used in the Siesta run: a double zeta polarized basis set (DZP) and the Perdew–Zunger exchange–correlation potential.

reduce the number of dominant products. For instance, figure 8 shows a converged spectrum of benzene in which the basis of dominant products is kept 7 times smaller than original basis of localized products. To judge the discretization error χ_0 , we provide a reference spectrum, computed in the basis of products of molecular orbitals $\varphi_E(\mathbf{r})\varphi_F(\mathbf{r})$ [6, 23] without any discretization. Due to unfavourable scaling behavior, such a reference calculation is only possible for sufficiently small molecules like benzene or naphthalene.

V. CONCLUSIONS

In this paper we have given an efficient construction of the Kohn–Sham response function for molecular systems. To find χ_0 , we made use of a previously found basis in the space of orbital products where χ_0 acts as a frequency dependent matrix. Our construction makes extensive use of fast Fourier techniques and it requires $O(N^2N_\omega)$ operations for N atoms on a lattice of N_ω frequencies. Two approximations were made: a basis was chosen in the space of orbital products with an error that vanishes exponentially in its size and the electronic spectral densities were discretized.

We tested our construction directly on exact results for χ_0 and by calculating electronic excitation spectra. The comparison with the exact but slow representation of χ_0 showed good accuracy of our construction. The excitation spectra from the Petersilka–Gossmann–Gross equations agreed with those of Casida’s equations. Moreover, an iterative Lanczos procedure allowed us to maintain $O(N^2N_\omega)$ scaling also for electronic excitation spectra. In this approach, the CPU time grows less steeply than in the solution of Casida’s equations that requires $O(N^3)$ operations. The

scaling of the Quantum Espresso method remains unpublished, but it is likely to be $O(N^2)$, according to one of its authors [24].

Our construction of χ_0 should have applications to excitons in polymers or organic semiconductors where the Coulomb interaction is poorly screened, and for implementing the GW approximation in molecular physics in a straightforward way. It is also planned to use our algorithm for the spectroscopy of surface adsorbed dyes.

Acknowledgements

It is a pleasure to thank James Talman (University of Western Ontario, New London) for contributing two crucial algorithms to this project, for making unpublished computer codes of these algorithms available to us, and for many fruitful discussions.

D.F. is grateful to Peter Fulde for extensive and continued support and for inspiring visits at MPIPKS, Dresden that provided perspective for the present work. Part of the collaboration with James Talman was done in the pleasant environment of MPIPKS.

D.F. acknowledges the kind hospitality extended to him by Gianaurelio Cuniberti and his collaborators at the Nanophysics Center of Dresden.

Both of us are indebted to Daniel Sanchez (DIPC, Donostia) for strong support of this project and for advice and help on the Siesta code.

We also thank Andrei Postnikov (Paul Verlaine University, Metz) for useful advice.

Olivier Coulaud of the NOSSI project and (INRIA, Bordeaux) helped with the Lanczos algorithm and by reading the manuscript. Our colleagues in this project, Ross Brown and Isabelle Baraille (both at IPREM, Pau), Nguyen Ky and Pierre Gay (both at DRIMM, Bordeaux), and Alain Marbeuf (CPMOH, Bordeaux) have contributed with many useful discussions.

We thank Mark E. Casida and Bhaarathi Natarajan (Joseph Fourier University, Grenoble) and their colleagues at Centro de Investigacion, Mexico for letting us use their deMon2k code and for much help with it. Our special thanks go to Mark E. Casida for his pertinent comments on our manuscript.

We also thank Stan van Gisbergen's (Vrije Universiteit, Amsterdam) for a trial licence of ADF.

This work was financed by the French ANR project "NOSSI" (Nouveaux Outils pour la Simulation de Solides et Interfaces). Financial support and encouragement by "Groupement de Recherche GdR-DFT++" is gratefully acknowledged.

-
- [1] *A Primer in Density Functional Theory*, edited by C. Fiolhais, F. Nogueira, M. A. L. Marques (Springer, Berlin, 2003).
- [2] *Time-Dependent Density Functional Theory*, edited by M. A. L. Marques, C. A. Ullrich, F. Nogueira, A. Rubio, K. Burke, E. K. U. Gross (Springer, Berlin, 2008).
- [3] A. L. Fetter, J. D. Walecka, *Quantum Theory of Many-Particle Systems* (McGraw-Hill, New York, 1971); H. Bruss and K. Flensburg, *Introduction to Many-body quantum Theory in condensed matter physics* (Copenhagen, 2003); I. Ye. Abrikosov, A. A. Gor'kov, L. P. Dzyaloshinskii, *Quantum field theoretical methods in statistical physics* (Oxford, Pergamon, 1965).
- [4] L. Hedin, Phys. Rev. **139**, 796 (1965).
- [5] M. Petersilka, U. J. Gossmann, and E. K. U. Gross, Phys. Rev. Lett., **76**, 1212 (1996).
- [6] M. E. Casida, in *Recent Advances in Density Functional Theory*, edited by D. P. Chong (World Scientific, Singapore, 1995), p. 155.
- [7] M. Rohlfing and S. G. Louie, Phys. Rev. Lett. **81**, 2312 (1998); for recent work, see L. Tiago and J. R. Chelikowsky, Phys. Rev. **B 73**, 205334 (2006). We thank Brice Arnaud (University of Rennes) for calling the latter paper to our attention.
- [8] W. Kohn, Y. Meir, and D. E. Makarov, Phys. Rev. Lett. **80**, 4153 (1998); For recent work, see for example J. Gräfenstein and D. Cremer, J. Chem. Phys. **130**, 124105 (2009); J. Toulouse, I. C. Gerber, G. Jansen, A. Savin, and J. G. Ángyán, Phys. Rev. Lett. **102**, 096404 (2009).
- [9] H. N. Rojas, R. W. Godby and R. J. Needs, Phys. Rev. Lett. **74**, 1827 (1995); L. Caramella, G. Onida, F. Finocchi, L. Reining, and F. Sottile, Phys. Rev. **B 75**, 205405 (2007).
- [10] J. E. Harriman, Phys. Rev. **A 34**, 29 (1986).
- [11] P.L. de Boeij, in *Time-Dependent Density Functional Theory*, edited by M. A. L. Marques, C. A. Ullrich, F. Nogueira, A. Rubio, K. Burke, E. K. U. Gross (Springer, Berlin, 2008); G. Te Velde, F. M. Bickelhaupt, E. J. Baerends, C. Fonseca Guerra, S. J. A. van Gisbergen, J. G. Snijders, T. Ziegler, J. Comput. Chem. **22** 931 (2001).
- [12] D. Foerster, J. Chem. Phys. **128**, 034108 (2008). The implementation of the method proposed in this paper has been improved thanks to a new algorithm: J. D. Talman, Int. J. Quant. Chem. **107**, 1578 (2007).
- [13] F. Aryasetiawan and O. Gunnarsson, Phys. Rev. **B 49**, 16214 (1994); A. Stan, N. E. Dahlen, and R. van Leeuwen, J. Chem. Phys. **130**, 114105 (2009).
- [14] P. Fulde, *Electron Correlations in Molecules and Solids*, Springer Series in Solid-State Sciences (Springer, Berlin, 1995) Vol. 100.
- [15] W. H. Press, S. A. Teukolsky, W. T. Vetterling, B. P. Flannery, *The Art of Scientific Computing* (Cambridge University Press, 1993).

- [16] P. Ordejón, E. Artacho and J. M. Soler, Phys. Rev. **B 53**, R10441 (1996); J. M. Soler, E. Artacho, J. D. Gale, A. García, J. Junquera, P. Ordejón, D. Sánchez-Portal, J. Phys. **C 14**, 2745 (2002). We used Siesta version 2.0.1 in this paper.
- [17] W. Kohn and L. J. Sham, Phys. Rev. **140**, 1133 (1965).
- [18] M. A. Blanco, M. Flórez, M. Bermejo, J. Mol. Struct. (THEOCHEM), **419**, (1997) 19–27.
- [19] J. D. Talman, J. Chem. Phys. **80**, 2000 (1984); J. Comput. Phys. **29**, 35 (1978); Comput. Phys. Commun. **30**, 93 (1983); Comput. Phys. Commun. **180**, 332 (2009).
- [20] V. I. Lebedev, Russ. Acad. Sci. Dokl. Math. **50**, 283 (1995). <http://www.ccl.net/cca/software/SOURCES/FORTRAN/Lebedev-Laikov-Grids/>
- [21] Y. Saad, *Iterative Methods for Sparse Linear Systems*, (Siam, Philadelphia 2003).
- [22] The Grenoble development version of deMon2k which is based upon deMon2k, version 2.2, A.M. Köster, P. Calaminici, M.E. Casida, R. Flores-Moreno, G. Geudtner, A. Goursot, T. Heine, A. Ipatov, F. Janetzko, J.M. del Campo, S. Patchovskii, J.U. Reveles, D.R. Salahub, A. Vela, The deMon Developers, Cinvestav, Mexico (2006); <http://dcm.ujf-grenoble.fr/PERSONNEL/CT/casida/deMonaGrenoble>.
- [23] R. M. Martin, *Electronic structure: basic theory and practical methods*, (Cambridge University Press, 2004).
- [24] R. Gebauer, private communication.
- [25] D. Rocca, R. Gebauer, Y. Saad, and S. Baroni, J. Chem. Phys. **128**, 154105 (2008).
- [26] The Fourier transform of this time ordered expression agrees with that of the retarded correlator at positive frequencies.
- [27] Atomic units are used throughout in this paper.
- [28] Energies are measured with respect to a “Fermi energy” – halfway between the LUMO and HOMO states
- [29] We use real spherical harmonics $S_{jm}(\mathbf{r})$ in our calculation to improve the performance.
- [30] We must apply $\chi_0(\omega)$ and f consecutively on vectors, rather than forming the matrix $1 - \chi_0(\omega)f$ which would require $O(N^3)$ operations. We assumed the dimension of the Krylov space to be of order $O(N^0)$, but we have not checked this in detail.